4thWLF 2017
4th World Landslide Forum
LJUBLJANA SLOVENIA EU

Simulation Model to Predict Landslide Speed Using Velocity-Dependent Viscous Damping

Eisaku Hamasaki, Hideaki Marui, and Gen Furuya

Abstract

We propose a simulation model using viscous damping to predict the moving velocity (v) of a landslide before it reaches a strain limit. We call this model "Lumped mass damper model", and it is based on a motion equation using a mass system model composed of a damper. The damper introduces a damping force in the opposite direction to the downward force (F) of the landslide, according to the landslide velocity. For slope-stability analysis, a simple model such as the Fellenius method is used. In the analysis, the resistance force (R) and driving force (D) are calculated in each individual slice and summed up for all slices. the safety factor (Fs) is indicated as Fs = R/D. Then, the equation of motion is shown as $m\alpha = F - A \cdot Cd \cdot v$. In the equation m is mass and α is acceleration of the landslide. After solving this motion equation, the formula '$v \approx F/A \cdot Cd$' is obtained. 'A' is the area of the slip plane of the landslide. 'Cd' is the viscosity coefficient of the damper, which exerts its effect on the slip surface of the landslide. Analytical results using this technique on the Kostanjek landslide in Croatia show that this Lumped mass damper model was able to reproduce the variations in landslide motion in response to the variation of groundwater level. Also, the Takino landslide of 4th August 1986 which was induced by embankment construction for a Japanese highway was successfully analyzed using this technique.

Keywords

Lumped mass damper model • Landslide • Moving velocity • Displacement • Damper • Mass system model

Introduction

The Saito model (1987) and Fukuzono model (1990) are well known models for predicting the final slope failure stages of landslide displacement from the collected data on earlier displacement velocity.

Although these models provide very useful results for the time of the final stage of slope failure after the tertiary creep stage, they do not consider the mechanical and physical state of the landslide bodies.

E. Hamasaki (✉)
Advantechnology Co., Ltd., 1-4-8-1202, Kakyouin, Aobaku, Sendai 9800013, Japan
e-mail: hamasaki@advantechnology.co.jp

H. Marui
Research Institute for Natural Hazards & Disaster Recovery, Niigata University, Niigata, 9502181, Japan
e-mail: maruihi@cc.niigata-u.ac.jp

G. Furuya
Engineering Department, Toyama Prefecturel University, Imizu, 9390398, Japan
e-mail: gfuruya@pu-toyama.ac.jp

M. Mikoš et al. (eds.), *Advancing Culture of Living with Landslides*,
DOI 10.1007/978-3-319-53498-5_67

Even though forces induced by such phenomena as rainfall, embankment and excavating may be increasing, the effects of these increasing forces are not considered in the analysis using these models.

Therefore, on the basis of the motion equation, a simulation model is proposed to predict the movement velocity (*V*) of the landslide before the strain limit of the sliding is reached. In order to predict the landslide velocity, an effective simulation model based on motion equations is proposed using a mass system model incorporating viscous damping.

The viscous damping is introduced to express a damping force, which acts in the opposite direction to the motion of the landslide, according to the landslide velocity. We call this model a 'viscous damper model' (or 'dashpot damper model' in Maxwell creep).

In the analysis, the resistance force (***R***) and driving force (***D***) are calculated for each individual slice and summed for all slices.

Although the safety factor (***Fs***) of thee slope stability analysis is indicated as '$Fs = R/D$', a downward force (***F***) is simply proposed as $F = D - R$. Here, if $Fs > 1$ then $F = 0$ is stable. On the other hand if $Fs < 0$ then $F > 0$ is unstable. Then, the equation of motion is shown as $m\alpha = F - k \cdot v$. Here, k is the 'dashpot damper'

The landslides to which this model can be applied are typically large slope movements, and not shallow landslides less than 2 m thick, rock falls or rapid small slope failures.

Furthermore the landslides that we treat by this model are generally of a slow movement type, with daily or hourly movement rates measured using monitoring devices such as extensometers, as in this research.

Simulation Model

Model Formula

Figure 1 shows the motion equation of the moving lumped mass damper model on the slope, as already described by Hamasaki et al. (2016).

As shown in Fig. 1, the equation of motion is applied to the calculated downward force (***F***), with the damper, $m\alpha$, calculated as follows:

$$m\alpha = F - kv \tag{1}$$

where,

m	Mass of the landslide body
α	Moving acceleration of the landslide
F	Downward force [$F = D - R$, $F > zero$]
k	Coefficient of dashpot [$k = ACd$]

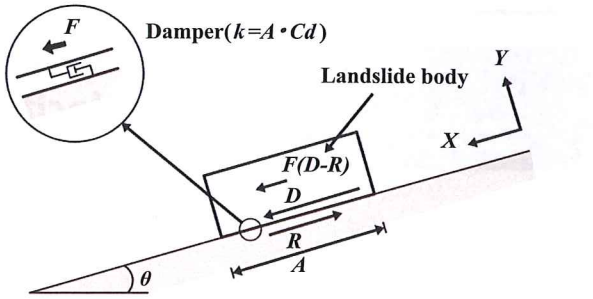

Fig. 1 Kinematic diagram of landslide body with damper (Hamasaki et al. 2016)

Cd	Coefficient of damper
v	Moving velocity of the landslide
D	Driving force [$=mg \sin\theta$]
R	Resistant force [$=(mg\cos\theta - u)\tan\varphi' + c'A$]
g	Gravitational acceleration
θ	Gradient of the slope
u	Pore-water pressure
c'	Cohesion of the slip surface
φ'	Internal friction angle of the slip surface
A	Area of the slip surface

In case of a cross section, 'A' means the length of the slip surface.

Dividing Eq. (1) by m, leads to the following formula:

$$\frac{dv}{dt} = \frac{F}{m} - \frac{k}{m} \cdot v \tag{2}$$

where

t	Time
dv/dt	Acceleration of the landslide[$=\alpha$]

Using the method of separation of variables in Eq. (2), and integrating both sides of the equation with respect to time, the landslide velocity is indicated by the following equation:

$$v = \frac{F}{k}\left(1 - e^{\frac{-k}{m}t}\right) \tag{3}$$

where, $k = A \cdot Cd$, Since Eq. (4) is as follows:

$$v = \frac{F}{A \cdot Cd}\left(1 - e^{\frac{-A \cdot Cd}{m}t}\right) \tag{4}$$

Moreover, even though the time (t) is short, the formula $e^{\frac{-A \cdot Cd}{m}t}$ is almost 'zero'. Hence, the velocity of the landslide is given approximately as:

$$v \approx \frac{F}{A \cdot Cd} \tag{5}$$

Equation (5) means that when $A \cdot Cd$ is constant, the landslide velocity increases or decreases in direct ratio to the downward force (Hamasaki et al. 2016).

Dumper Characteristic Depending on Velocity

Figure 2 shows the schematic creep image diagram for the relationship between the downward force (F) and displacement (X) of the landslide. Here, the velocity (v) varies in proportion to the downward force, F, as indicated in Eq. (5).

Based on this model, when F is less than zero, the velocity of the landslide is zero, hence the displacement X does not increase. However, when F is greater than zero, the displacement X begins to increase. During the duration of increasing v and F, the acceleration (α) is greater than zero. At the same time, the displacement X increases, as in tertiary creep. On the other hand, during a reduction of F (>0), the landslide slows at the same time. However, the X continues to increase while the rate of increase of X is reduced, as in primary creep. Moreover, when the value of F continues at a constant value greater than zero, the velocity v also remains constant. Therefore, the acceleration is zero and the speed remains constant as in secondary creep.

Model Validation

The Kostanjek Landslide Site

The Kostanjek landslide, located near the western part of the western hills of Zagreb, the capital City of Croatia, is a large, deep-seated translational landslide that is approximately 1000 m wide, with a maximum length of about 1300 m and an average length of about 1100 m. The maximum thickness of the landslide is about 70–90 m. On the landslide and in its surrounding areas there are many factories and houses as it is a suburb of the City of Zagreb. The geological features affecting the Kostanjek landslide are the distribution of Tripoli marl and the gentle slope of structural bedding planes. The landslide also has a gently sloping slip surface, with an average angle of 5°, and moves to the south-southwest while causing the toe part to rise by buckling upward (Fig. 3).

The direct cause of the landslide was removal of marl for use in a cement factory in the toe part of the landslide. This began in 1962 (Stanic and Nonveiller 1996). A tunnel for transporting the marl had been dug from the central portion to the head. In the boundary between stable bedrock and the moving landslide body, about 85–93 m from the mouth of the tunnel, a slip-surface clay with clear slickensides was observed. In addition, there were opening cracks and tilting of houses in the suburbs on the landslide boundary.

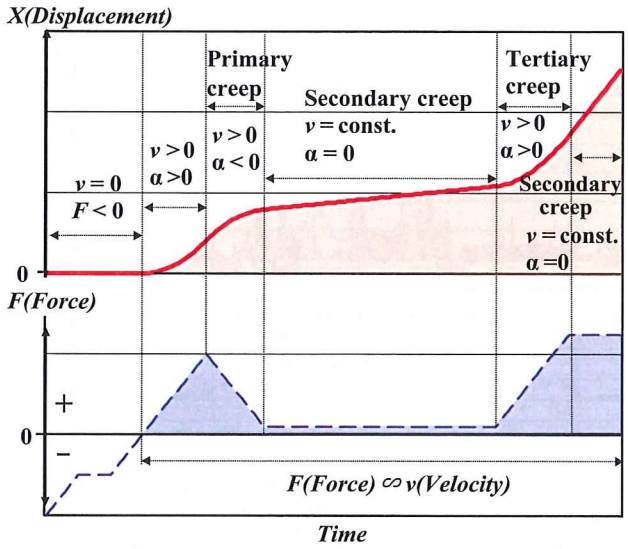

Fig. 2 Schematic diagram for relation between force (F) and displacement (X) (Hamasaki et al. 2016)

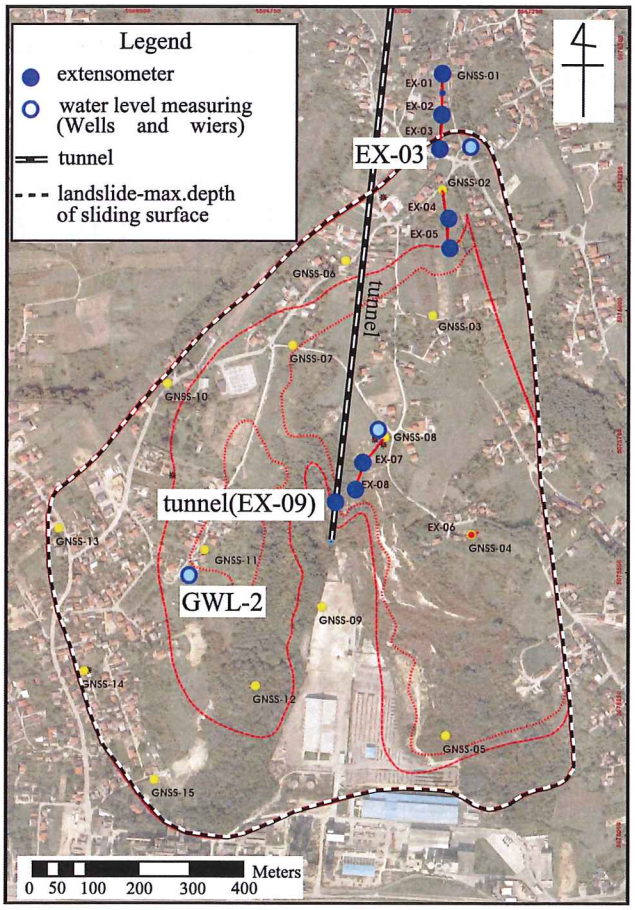

Fig. 3 Location map of landslide area and monitoring equipment

However, no counter-measures have ever been taken against the landslide (Furuya et al. 2011).

Landslide movement began in 1963, after the start of excavation of the marl. Excavation of a total amount 5.3×10^6 m^3 was completed in 1988. In the subsequent 25 years movement of 3–6 m of the landslide was confirmed (Stanic et al. 1996).

Moreover, in the 21 years following the excavation, movement of 0.75–1.6 m between 1988 and 2009 was measured (Marui et al. 2013). After 2009, some bore-hole monitoring equipment was installed from 2011 to 2013 using the SATREPS system of Japan. Extensometers and a global navigation satellite system (GNSS) for early warning were precisely installed in the landslide zone. A further extensometer (EX-09) was installed in the tunnel to the slip boundary portion. After this, as shown in Fig. 4, tensile displacements of the extensometers (EX-09 and EX-03) in the landslide, was gradually seen. Moreover, the downward movement of the GNSS was indicated. Especially since 2012, after continuous rainfall of 169 mm in 30 days, the displacement of the landslide has been increasing.

These average tension fluctuation have increased to 1–3 mm/day since around April 2013.

Furthermore, Fig. 4 shows that the displacement velocity of extensometer Ex-9 varies in proportion to the ground-water level fluctuations recorded in GWL-2 installed in the landslide.

Model Simulation of the Kostanjek Landslide

Figure 5 shows a lumped mass damper model of the Kostanjek landslide created in accordance with Fig. 1. In this case, the cross-section length A = 1100 m, the layer thickness D = 70 m, and the slip surface gradient $\theta = 5°$ are applied. Further, the saturated unit weight $\gamma sat = 19$ kN/m^3 and unsaturated unit weight $\gamma t = 18$ kN/m^3 were assumed for the marl in the landslide body. Furthermore, the unit weight of water was $\gamma w = 9.8$ kN/m^3. In addition, the cohesion and angle of internal friction on the slip surface adopted a $c' = 0$ kN/m^2 $\varphi' = 9°$ of residual strength (Stanic et al. 1996). The ground-water level of GWL-2 on September 12, 2012 was 57.88 m. Which was taken as the 'reference water level'.

This water level as the reference date, at the same time the head of water from the slip plane of the reference date applied 'zero' m as calculation model.

The hydraulic head from the slip plane when the landslide reached a critical state WL = 60.25 m (***Fs*** = 1.0) on September 21. In other words, the groundwater level in GWL-2 at this time was made to have a 2.37 m (=62.25–57.88) rise above the reference water head. Here, the value of ***Cd*** was calculated as 1.0×109 kN s/m (per m^2).

Based on the formula (5), the speed (***v***) and displacement (***X***) of the landslide were calculated using observed daily level variations in GWL-5 from September 12, 2012 to June

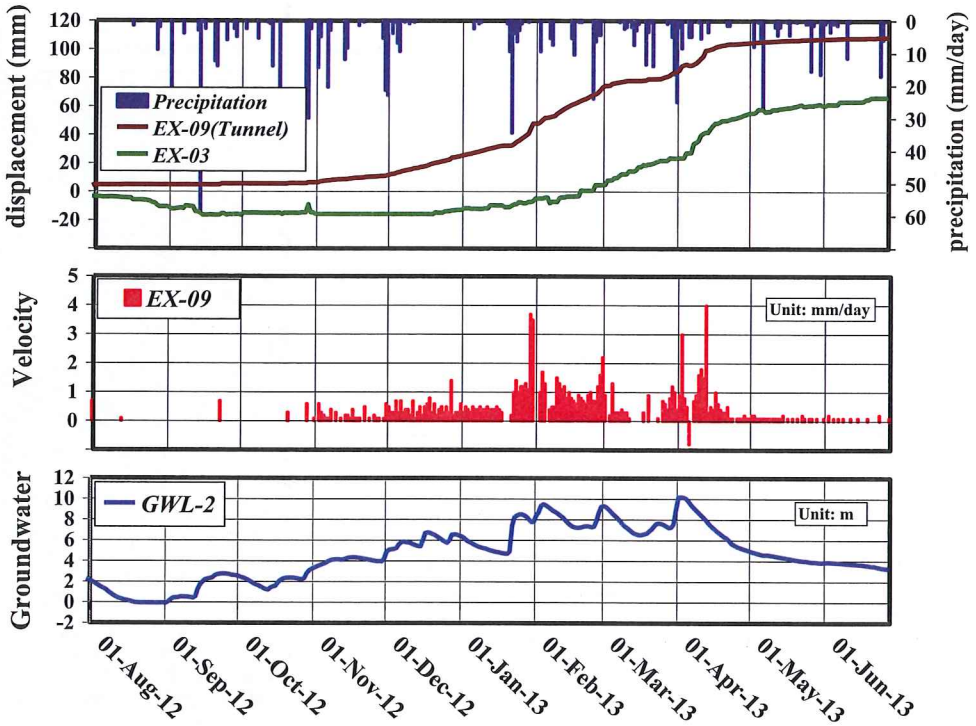

Fig. 4 Relation among monitoring data (daily precipitation, movement of EX-09 and EX-03 as extensometer, velocity of EX-09 and ground-water level of GWL-2) at Kostanjek landslide (Hamasaki et al. 2016)

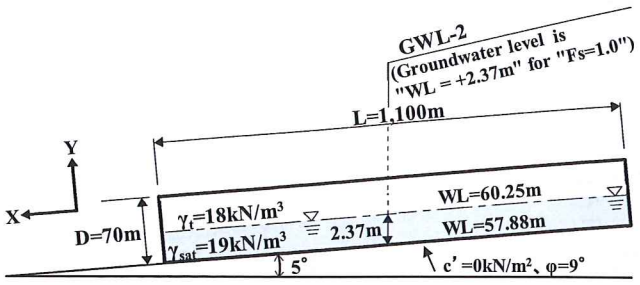

Fig. 5 Schematic diagram of slope stability analysis adapted for Kostanjek landslide

2013. Here, the safety factor (***Fs***) of the landslide was calculated as ***Fs*** = ***R/D***. The model calculation results are shown in Fig. 6.

Comparing the calculated values with the observed values of the displacement of extensometer EX-9 shows a slight difference in the final stage, but the overall trend is almost the same (Fig. 7). Especially since April, it is clearly understood that the movement velocity in both the observation and the calculation has shown a tendency to decline as ***F*** is reduced by the drawdown of GWL-2.

Moreover, the correlation coefficient exhibits a high value of 0.88. Further it has been shown mean square error (RMSE) also 0.21 mm as small value per day. Figure 7 shows these results.

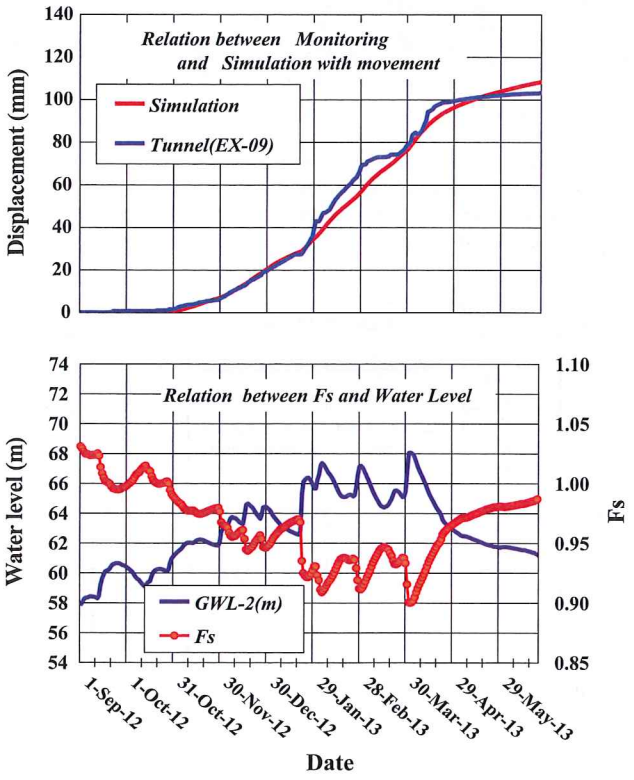

Fig. 6 Reproduction of landslide displacement by two dimensional model. Diagram shows relation between result (Simulation and Fs) and monitoring data (EX-09, GWL-2) at Kostanjek landslide area

The Takino Landslide Site

The Takino landslide occurred on 5 August 1986 in Iwate prefecture in northern Japan, after a rainfall in excess of 300 mm in two days. The landslide was a large one, with a length of about 230 m, a width of 250 m and a thickness of over 20 m. The bedrock consists of Neogene tuff. The head of the landslide included an embankment of a highway construction that was almost finished for opening in November 1986.

The heavy rain was the direct trigger of the landslide.

However, the maximum factor to induce the landslide was the embankment fill loaded on the head part of the landslide. After August 5, the landslide was found to be moving more than 10 mm/day. Emergency remedial works were rapidly carried out. By August 20 removal of soil had reduced the embankment by 5.4 m in height. After that, the landslide was almost stopped (Fujino et al. 1989). Figure 8 shows the main geological profile of the Takano landslide.

Model Simulation of the Takino Landslide

Fujino et al. (1989) summarized the relation between the data on the displacement velocity and the height reduction of the embankment from the emergency counter measures period at the Takino landslide. From the 21 m depth of movement on the slip surface obtained by the strain gauge installed in the H steel piles, the slip plane can be estimated.

The geological cross-sectional view is given in Fig. 8. In order to reproduce the landslide velocity, we compared the

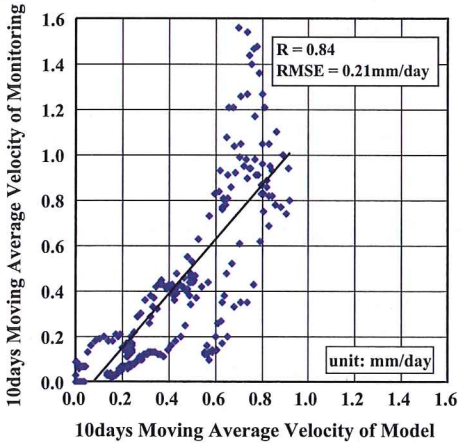

Fig. 7 Comparison between monitoring data and simulation data for 10-days moving average velocity of EX-09 at Kostanjek landslide area

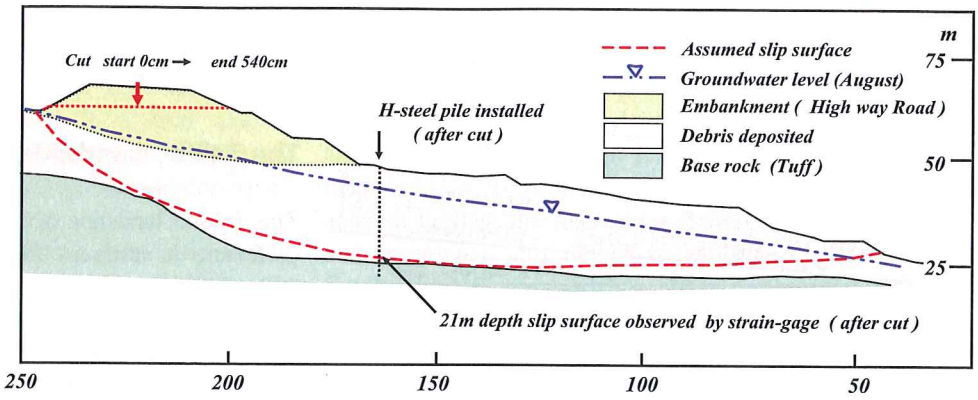

Fig. 8 Main geological cross section of the Takeno landslide (Fujino et al. 1989)

Fellenius method for slope stability analysis and this lumped mass damper model. Here, it is noted that no change in the groundwater level is taken into consideration. As the embankment at the head of the landslide, is removed step by step, the stability of the landslide should not only be increasing but its velocity should be decreasing. Through such understanding, the Fellenius method, which is calculated using accumulated slices was applied with $\gamma t = 18$ kN/m^3 as the unit weight, $c' = 20$ kN/m^2 as the cohesion, and $\varphi = 9.5°$ as the internal friction angle. These settings for the slip-surface strength were determined by back-calculation from the embankment removal for the case Fs = 1.0 which was a critical point on 18 August. In addition, ***Cd*** was set for 1.08×10^9 kN s/m (per m^2).

Figure 9 shows relationship between the monitoring and the simulation for the velocity and displacement of the landslide. After 8 August, the safety factor (***Fs***) is over 1.0, because the amount of cut is enough. Therefore, since then, the velocity is zero. In addition, before then, the trend between the monitoring and the simulation for the velocity and the displacement were very similar. In other words, this Lumped mass damper model proved to be useful to predict the landslide velocity for not only a landslide induced by increasing water pressure but also for a landslide induced by the surcharge load of an embankment at the head part of a landslide.

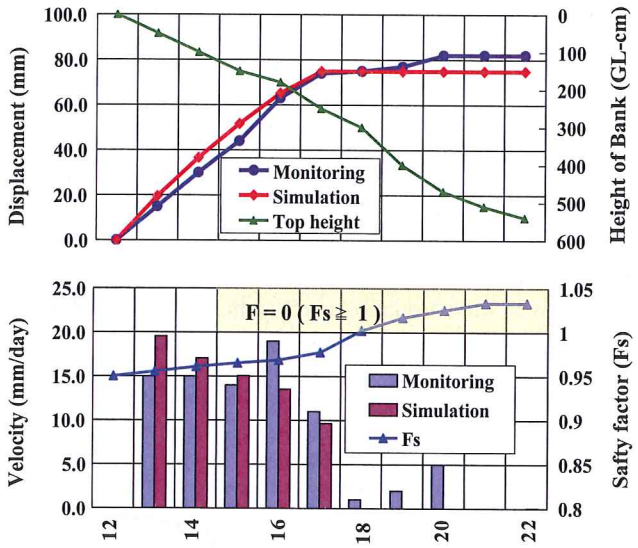

Fig. 9 Relation between monitoring and simulation for velocity and displacement. Furthermore, the figure shows the decreasing elevation (GL-m) of the top of the cut surface and the safety factor of the landslide for each step

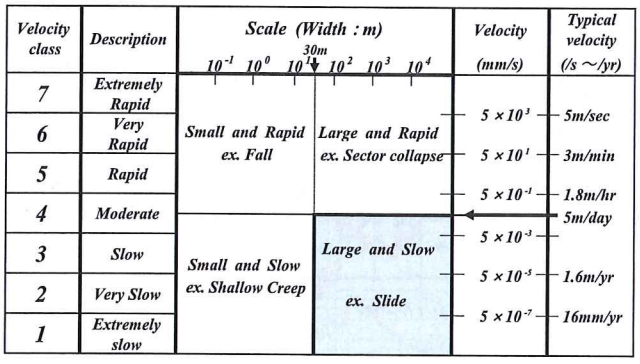

Fig. 10 Landslide classification diagram using relation between velocity and scale (Oyagi 2004)

Discussion

Landslide Types Analyzed in This Model

This "Lumped mass damper model" is applied to slow and large scale landslides that have thin clay layer of slipping and thick rigid mass of moving. Oyagi (2004) classified landslides using the relation between moving velocity and scale as shown in Fig. 10. According to this figure, this damper model can be applied to 'Slide type (Large and Slow)', which has less 5 m/day of velocity and over 30 m width.

In addition, Watari (1986) described that such 'Slide' type landslides have thin clay layer along the slip surface and thick rigid mass, both of which consist a whole landslide body

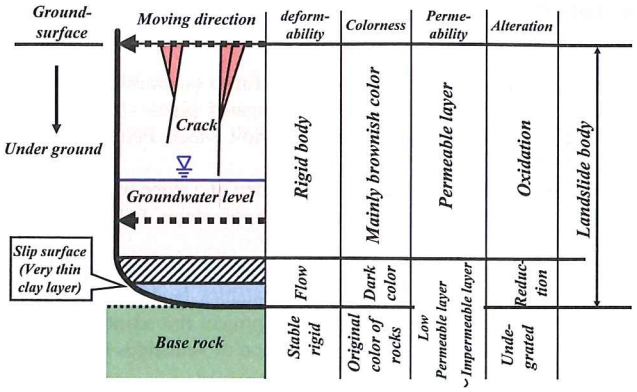

Fig. 11 Conceptual partial cross section diagram of 'Slide type' in landslide (Watari 1986)

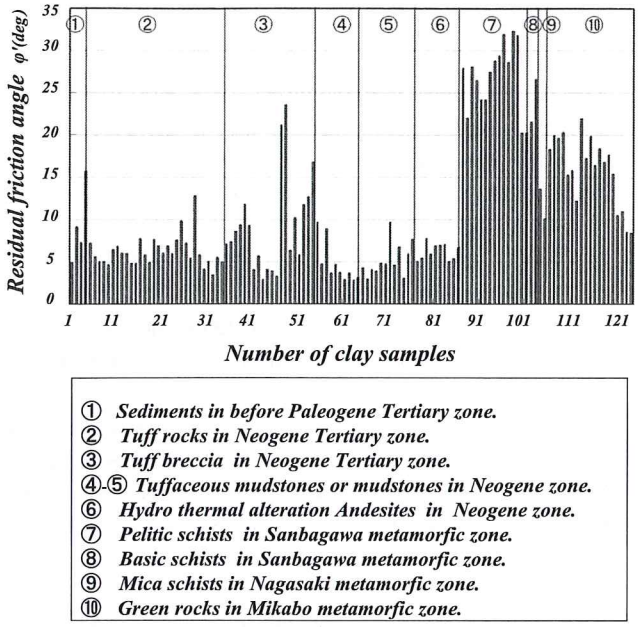

Fig. 12 Residual friction angle ($\varphi r'$) results of slip surface clay from repetitive shear tests on several geological type in Japan (Mayumi et al. 2003)

(Fig. 11). He explained that the deformation of slip-surface clay is responsible for much of the landslide displacement on the basis of many analytical examples. Particularity, there are lots of 'Slide type' landslides in Neogene zone in Japan. It is well known that these landslides have gentle slope inclination and very weak strength of slip surface.

Mayumi et al. (2003) gained residual strength values from 124 samples of repetitive shear test results of various slip surface clays from many landslide areas in Japan (Fig. 12). Figure 12 shows the test results of residual friction angle of these landslide clays. The values of residual friction angle less than 10 degrees occupied over 60% of all test results. Especially, the average of these angle is between 5° and 9° for the slip surface clay in Neogene zone.

In fact, the both Konstanjek landslide and Takinosawa landslide have the value of residual friction angle less than 10°, and have the thick rigid bodies compared with these thin slip layers like Watri's model. Therefore, it is reasonable that this damper model was applied to the two cases, namely the Konstanjek landslide, the Takinosawa landslide. Moreover, It is appropriate to set our goal to know the velocity of landslide movements from common slope stability analysis on the basis of the fact that most of slope stability analyses are derived from consideration of balance of forces acting on rigid bodies.

Model Characteristics

The two important points in this lumped mass damper model are (1) it has a viscous resistance (=damper $\boldsymbol{k}$), which is proportional to landslide speed, which contributes to the dissipation of kinetic energy; (2) if the value of the damper k ($=\boldsymbol{Cd\,A}$) is constant, the velocity ($\boldsymbol{v}$) increases or decreases in proportion to the downward force ($\boldsymbol{F} \geqq 0$) of the landslide.

The Kostanjek landslide has yet to collapse even though it reached up to the early tertiary creep stage. It is well known that many landslides lead to slope failure by increasing their moving velocity, even without increasing downward force in the tertiary creep stage. What that means is the displacements of those landslides have exceeded their strain limit. The landslide need not exceed the 2 mm/h of Japan's warning criteria because it was up to 3 mm/day. The amount of displacement of the Kostanjek landslide did not reach the strain limit because it did not exceed the hourly maximum fluctuation of 2 mm.

Therefore, conditions that lead to such extreme strain limit stage are one of the future key issues. Two possible assumptions in order to estimate the extreme strain limit stage are indicated as follows.

One is a decrease in shear strength or $\boldsymbol{Cd}$-value itself on the slip surface due to exceeding the strain limit stage. The second is a decrease in thickness with effective viscosity due to exceeding the strain limit stage. In addition, it is determined that this formula is useful as a predictive model in the movement long-medium term fluctuations of landslides. Further, there is a possibility that the damper model can be improved by combining it with the Fukuzono model (2001) or the Saito model (1981) as a short-term slope-failure prediction model. Also in the future, we can expect to understand the physical meaning of the damper applied to landslides through several tests such the shear test.

Conclusion

1. The lumped mass damper model '$v \approx F/A\ Cd$' is very simple formula, which implies that if the value of the damper k ($=A\ Cd$) is constant, the velocity (v) increases or decreases in proportion to the downward force (here, $F \geqq 0$) of the landslide.
2. In addition, the lumped mass damper model is a useful method to predict the velocity of landslides caused by increasing water pressure, and for landslides induced by terrain modification such the building of an embankment or an excavation.
3. In the future, in order to predict the time of a slope failure, an improved model will be considered to combine with other creep slope failure models, such as the Fukuzono model (2001) or the Saito model (1981).

Acknowledgements First, we would like to acknowledge the late Dr. Hiroyuki Yoshimatsu, who gave us the opportunity to study landslides, and many rich research experiences. We are also grateful to the members of the SATREPS project in Croatia, Prof. Kyoji Sassa, Prof. Toyohiko Miyagi, Dr. Osamu Nagai, Dr. Chunxiang Wang, Mr. Takeshi Kato and the Croatian members: they provided at all levels of the research project. Last, I wish to thank Haruna Ishikawa for support in writing this article.

References

Fujino T, Okuzono S, Uchibori S (1989) Effect on landslide control by light weight embankment with corrugated pipes—Ichinohe landslide area of Tohoku Expressway. Soil Mech Found Eng 37–2 (373):19–24 (in Japanese)

Fukuzono T (1990) Prediction of failure time of a slope by reciprocal of mean velocity—study on prediction of slope failure, p 3 (in Japanese)

Furuya G, Migagi T, Hamasaki E, Krkac M (2011) Geomorphological mapping and 3D modeling of the Kostanjek landslide, Zagreb. In: Proceedings of 2nd workshop of the project risk identification and land-use planning for disaster mitigation of landslides and floods in Croatia. Rijeka, Dec 2011

Hamasaki E, Marui H, Yoshimatsu H, Kato T, Furuya G, Wang C (2016) Lumped mass damper model to predict landslide velocity. J Jap Land Soc 56(4):128–133 (in Japanese)

Marui H, Yoshimatsu H, Hamasaki E, Katou T, Wang C (2013) JJapanese-croatian joint research project for disaster mitigation of landslides and floods. J Water Sci (Japan) 332:146–167 (in Japanese)

Saito M (1987) Application of creep curve to predict slope failure time. J Jap Land Soc 24(1):30–38 (in Japanese)

Stanic B, Nonveiller E (1996) The Kostanjek landslide in Zagreb. Eng Geol 42:269–283

Yoshimatsu H, Hamasaki E, Marui H, Kato T, Wang C, Krka M, Mihali Arbanas S (2013) Characteristics of sliding displacement of Kostenjak landslide in Croatia. In: Abstract proceedings of the 4th Croatian-Japanese project workshop, Split, Croatia, University of Split, Faculty of Civil Engineering, Architecture and Geodesy, pp 29–29